

# Ultraviolet structure in the lensed QSOs 0957+561<sup>1 2</sup>

J.B. Hutchings

Herzberg Institute of Astrophysics, NRC of Canada,  
Victoria, B.C. V9E 2E7, Canada; john.hutchings@nrc.ca

Received \_\_\_\_\_; accepted \_\_\_\_\_

arXiv:astro-ph/0303544v1 24 Mar 2003

---

<sup>1</sup>Based on observations with the NASA/ESA *Hubble Space Telescope*, obtained at the Space Telescope Science Institute, which is operated by AURA Inc under NASA contract NAS5-26555

<sup>2</sup>Guest User, Canadian Astronomy Data Centre, which is operated by the Dominion Astrophysical Observatory for the National Research Council of Canada's Herzberg Institute of Astrophysics

## ABSTRACT

Imaging and spectra of the lensed QSO pair 0957+561 are presented and discussed. The data are principally those from the STIS NUV MAMA, and cover rest wavelengths from 850Å to 1350Å. The QSOs are both extended over about 1 arcsec, with morphology that matches with a small rotation, and includes one feature aligned with the VLBI radio jets. This is the first evidence of lensed structure in the host galaxy. The off-nuclear spectra arise from emission line gas and a young stellar population. The gas has velocity components with radial velocities at least 1000 km s<sup>-1</sup> with respect to the QSO BLR, and may be related to the damped Ly $\alpha$  absorber in the nuclear spectra.

*Subject headings:* galaxies: active – galaxies: quasars: individual (Q0957+561)

## 1. Introduction and observations

Q0957+561 is a bright gravitationally lensed QSO pair at redshift 1.415. The two images are 6.2" apart, and deep imaging reveals a chief lensing galaxy between them, which lies in a cluster at redshift 0.36. The lensing model and QSO host galaxy morphology have been discussed recently by Keeton et al (2000), and their paper contains a good bibliography of related earlier work. The QSO UV spectra reveal that they have damped Ly $\alpha$  absorption and other associated absorbers that arise in the QSO host galaxy (see Michalitsianos et al 1997, and Dolan et al 2000). Repeated UV nuclear spectroscopy has revealed changes and differences in the UV absorbers that are discussed in the above references.

In order to look for extended Ly $\alpha$  in the vicinity of the QSO, and to study the structure of the nuclear regions, direct images and slitless spectra were taken with the NUV detector of the Space Telescope Imaging Spectrograph (STIS). Both QSO images were in the field of view. Table 1 summarizes the observations, and also others taken with the same STIS grating, which were obtained from the HST archive. This paper discusses the non-nuclear spectra and UV imaging, which have not been covered in the other work referred to above.

## 2. UV images

The UV images are shown in Figure 1, along with images of stars taken with the same detector. For comparison, several star images, with exposure times and signal levels similar to the QSO images, were taken from the HST archive. While the star images all show deviations from circular symmetry, due to HST tracking jitter, they are all smaller and rounder than the QSO images, as can be seen in Figure 1 and also from the luminosity profiles in Figure 2. Figure 3 shows contours of the two QSO images.

Figure 1 shows both QSOs, rotated to the conventional orientation, the most

non-circular star image, and the average image from several stars. The images have been smoothed with a gaussian of  $\sigma=2$  ‘pixels’ (0.025”) to reduce the granularity of the photon-counting MAMA detector, but this does not significantly affect the spatial resolution (FWHM about 5 pixels) which is determined by the HST optics. The QSOs both have very similar ‘kidney-shaped’ inner profiles, and fainter radial structures, and match each other best with a small relative rotation, depending on whether the cores or radial spokes are fit. No such structure is seen in any star image, and the jitter in the QSO observation does not indicate a difference from the star observations. Thus, we conclude that there is resolved structure in the inner 0.3 arcsec diameter of the QSO images, and that the lensing distortion and rotation within this spatial scale is small. The radial structures are seen out to distances of about 0.4 arcsec, and do show larger differences in extent and relative brightness.

The luminosity profiles are derived from the IRAF ‘ellipse’ task, and plot the semi-major axis of the best fit ellipse to each signal level. The star profile is the mean profile from all the star images. The two spatial axis plots show that these inner profiles are not exponential or power-law. The QSO profiles are resolved at essentially all radii: the kink in the star profiles is caused by the HST PSF structure that shows up most clearly in the unresolved stellar images. We can also see that the B image is larger than the A image in the inner parts (by some 20% in radius, normalised to the peaks). The B image is brighter, but only by 1%, as the peak signal is lower. We discuss the image morphology in the last section.

There is no sign of the lensing galaxy or any other object in the 25 arcsec field of the UV image, as expected for the redshifted SED of a cluster galaxy at redshift 0.36. The only WFPC2 images of the QSOs have 0.1” pixels and show no resolved structure, but do reveal the lensing galaxy.

### 3. Slitless spectra

The dispersed image contains spatially resolved spectra of both QSO images. As these have no wavelength calibration, it was necessary to process the raw image into one with spatial and wavelength axes, separately for each QSO. The wavelength scale was established by using the nuclear emission lines and assuming the QSO emission-line redshift of 1.415. These are described together with the standard long-slit spectra (see Table 1) in the next section. Figure 4 shows the nuclear spectra, and off-nuclear spectra, also described in the next section. As the nuclear UV spectra have been discussed in detail by the papers noted above, this paper does not investigate them further.

The dispersed image was inspected carefully for signs of Ly $\alpha$  emission elsewhere in the field. This might arise from emission-line gas at the QSO redshift (i.e. associated with the host galaxy), either on the scale of the host galaxy, or close to the QSO nucleus. The lensing of the QSO and environments means that this may be found anywhere between the two QSO nuclei and at some distance beyond. The background is remarkably uniform, and no significant extra flux is seen in the likely regions, compared with the rest of the image. Close to the nuclei, Ly $\alpha$  emission is not noticeably extended beyond the rest of the UV continuum. Thus, the data do not reveal any detached Ly $\alpha$  emission line gas around the QSO.

### 4. QSO off-nuclear spectra

The cross-sections of the UV spectra are shown in Figure 5. The resolved width of the nuclear regions cause the slitless spectra to be wider than the 0.2" slit spectra. Further, the extended structure seen in the UV images in Figure 1, will give rise to more off-nuclear signal in the slitless spectra. Both these are seen. The closest comparison is between

the two spectra of QSO A with dispersion angles  $110^\circ$  and  $114^\circ$ . There are additional uncertainties in the exact positioning of the nuclear region with the 0.2" slits.

It was found that the regions outside 0.1" in the slit spectra and outside 0.21" in the slitless spectra are free of nuclear contamination, by noting that they do not show the damped Ly $\alpha$  absorption. The regions inside that in the slitless spectra (dotted lines in Figure 4), are slightly contaminated, and Figure 3 shows the effect of subtracting a scaled nuclear spectrum just sufficient to remove the damped Ly $\alpha$  absorption.

The off-nuclear spectra for components A and B in the slitless data are very similar, extracted as shown in Figure 5. Thus, Figure 3 shows the combined A+B spectra. There is clearly off-nuclear Ly $\alpha$ , which we discuss in more detail below, but we also note the possible presence of N V (1238-42Å), and an associated UV continuum, which has the same spatial extent as the line emission. Both suggest the presence of a young stellar population. Extraction of off-nuclear spectra from the G430L and G750L observations (see Table 1), shows a noisy broad emission at redshifted C IV (1550Å) which also suggests a distributed young population. At longer wavelengths, the off-nuclear spectra have a flatter (i.e. redder) SED, which presumably arises from an older stellar population as well. At the QSO redshift, we can see rest wavelengths out to about 4000Å, but the signal is too weak and noisy to reveal line features.

Figure 6 shows the Ly $\alpha$  emission separately for all off-nuclear spectra, and both QSO components. The combination of the spatial extent of the off-nuclear emission-line regions, the slit width (or lack of slit), and the uncertain placement of the nucleus within the slit, make velocity measures of the line rather hard to interpret. However, the width and offset of the lines from the QSO redshift (shown dotted in) indicates that some Ly $\alpha$  emission gas has velocities at least of order  $1000 \text{ km s}^{-1}$  with respect to the nucleus. The W spectra at all orient angles indicate redshifted emission that corresponds to radial velocities of several

thousand  $\text{km s}^{-1}$ . As noted above, the behaviour in components A and B is similar and suggests that the lensing does not distort the spatially resolved near-nuclear regions very much.

## 5. Discussion

The far-UV rest-frame imaging and spectra of Q0957+561 show that the QSOs are resolved over scales of about 1 arcsec, and that the two lensed components have very similar morphology out to radii of 0.3 arcsec, although component B is larger by about 20%. There are also fainter radial features that extend over diameters of 1.5 arcsec, that do show differences between A and B. There is no sign of the lensing galaxy, or of more extended  $L\alpha$  in the UV data.

The radio structure is of interest, and known to comparable spatial resolution. Conner, Lehar, and Burke (1992) published VLBI maps that resolve jets from both A and B over some 100mas. Garrett et al (1994) show these in more detail, and there is larger structure mapped with the VLA by Greenfield, Roberts, and Burke (1985). The 100mas jets are at position angles  $23^\circ$  and  $17^\circ$  for A and B, respectively, although they are both near  $14^\circ$  in the inner 10mas, and the A jet curves to PA nearly  $90^\circ$  over 5 arcsec. The radio flux magnification (B/A) is close to 0.75 (see e.g. Press and Rybicki 1998), while the optical values are near to unity. This disagreement is considered to be due to microlensing, or possibly the nearness of B to a lensing caustic.

The UV images reported here do have an extension with position angle about  $25^\circ$ , over the innermost 100mas, which suggests that they are associated with the radio jets. They do also have extensions with similar size, but less sharpness, at angles  $-60^\circ$  and  $-170^\circ$ , as seen in Figure 3. The best fit between A and B over the inner 200mas radius is with a  $4.5^\circ$  rotation

clockwise of B, which is the opposite direction of the radio jet angle differences. As noted, the UV flux magnification is 1.01 and the size is 1.2 (both B/A). Thus, it appears that some of the UV structure is aligned with the radio jets, but the difference in magnification is similar to that at optical wavelengths.

The off-nuclear spectra indicate that there are clouds of emission line gas within the QSO host galaxy with relative velocities of the order of  $1000 \text{ km s}^{-1}$ , and possibly significantly higher. This suggests association with the damped absorber seen in the nuclear spectra, which indicates outflows of about  $2500 \text{ km s}^{-1}$ . The off-nuclear  $\text{Ly}\alpha$  flux is about  $10^{-12} \text{ erg s}^{-1}$ , (10% of the nuclear line BLR flux), and the equivalent widths similar to the nuclear at about  $70\text{\AA}$ . The off-nuclear spectra also indicate the presence of a young hot stellar population, as well as a redder population that begins to dominate above rest wavelengths  $4000\text{\AA}$ .

Further high resolution imaging and spectra should provide more information on the spatial structure, and possibly associate it with changes seen in the nuclear absorption spectra. The inner morphology also may provide further constraints on lensing models for the QSO.



Table 1. STIS UV observations of Q0957+561

QSO	Date d/m/y	Slit	Grating	exp (sec)	Orient <sup>a</sup> (deg)	Note
A	15/04/99	52x0.2	G230L	1900	81.9	also G430L,G750L
B	02/06/00	”	”	1900	49.6	also G430L,G750L
A	08/09/00	”	”	1500	–66.3	
A+B	10/03/01	open	25MAMA	200	109.7	
A+B	10/03/01	open	G230L	2200	109.7	

<sup>a</sup>Position angle of image y-axis degrees E of N

References

- Conner S.R., Lehar J., Burke B.F., 1992, *ApJ*, 387, L61
- Dolan J.F., Michalitsionos A.G., Nguyen Q.T., Hill R.J., 2000, *ApJ*, 539, 111
- Garrett M.A., Calder R.J., Porcas R.W., King L.J., Walsh D, Wilkinson P.N., 1994, *MNRAS*, 270, 457
- Greenfield P.E., Roberts D.H., Burke B.F., 1985, *ApJ*, 293, 370
- Keeton, C.R., et al, 2000, *ApJ*, 542, 74
- Michalitsianos A.G. et al, 1997, *ApJ*, 474, 598
- Press W.H., Rybicki G.B., 1998, *ApJ*, 507, 108

Captions to figures

1. UV images (rest frame 900-1300Å) of the QSOs (upper), compared with stellar images taken at the same observed wavelengths and detector (lower). Images are all 8" on a side, have similar signal levels, and the same display lookup table. The QSOs are oriented N up and E to the right. The left QSO image is component A and the right one is B. The left star is the ‘worst’ one found in the archive, and the right one is the composite of four stars. Note the similar core structure in the QSOs, larger than the stars, and also the radial faint rays emerging from the QSO images.

2. Radial profiles of the QSO images and the mean of the star images, plotted on  $R^{1/4}$  and  $R$  scales. The QSO images are extended, with the B image being larger, but with a very similar profile. Formal error bars from the ellipse task are plotted.

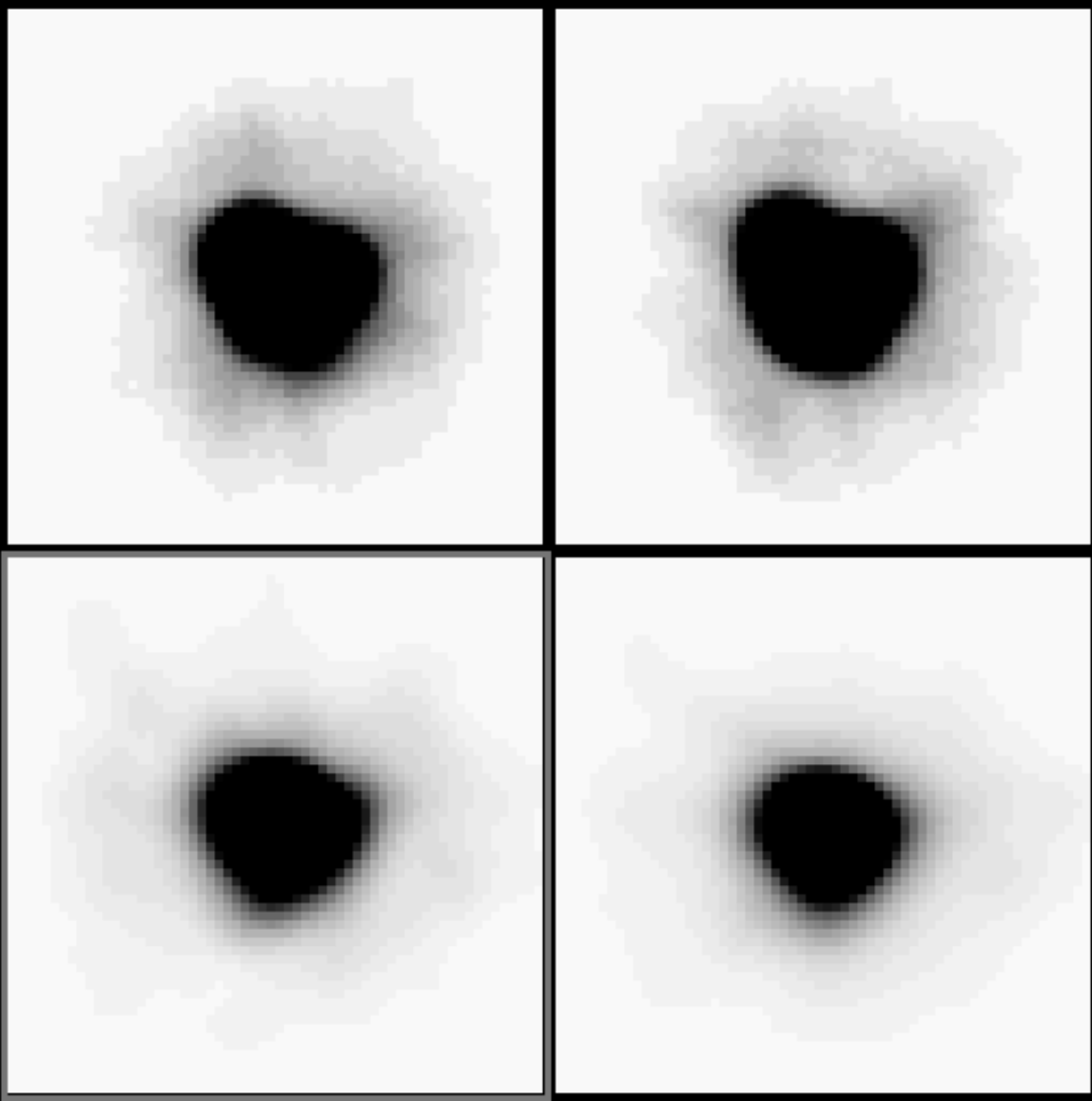
3. Contour plots of the two UV images. North is up and East to the left. The extension to the NE is aligned with the VLBI radio jets. The two images align best with a rotation of  $4.5^\circ$ .

4. Spatially resolved UV spectra of Q0957+561. The wavelength scale is the rest frame, and spectra step across the nucleus as shown in the cross sections in Figure 5. As the inner QSO structure (and the extracted spectra) are so similar, the off-nuclear spectra are combined from both A and B components. The central panel shows the two nuclear spectra (scaled down by some 20 times compared with the others). Note the small differences in the damped absorption lines. The two extractions nearest the nucleus are probably contaminated by nuclear light, and are also shown after nuclear subtraction sufficient to remove the Ly $\alpha$  absorption.

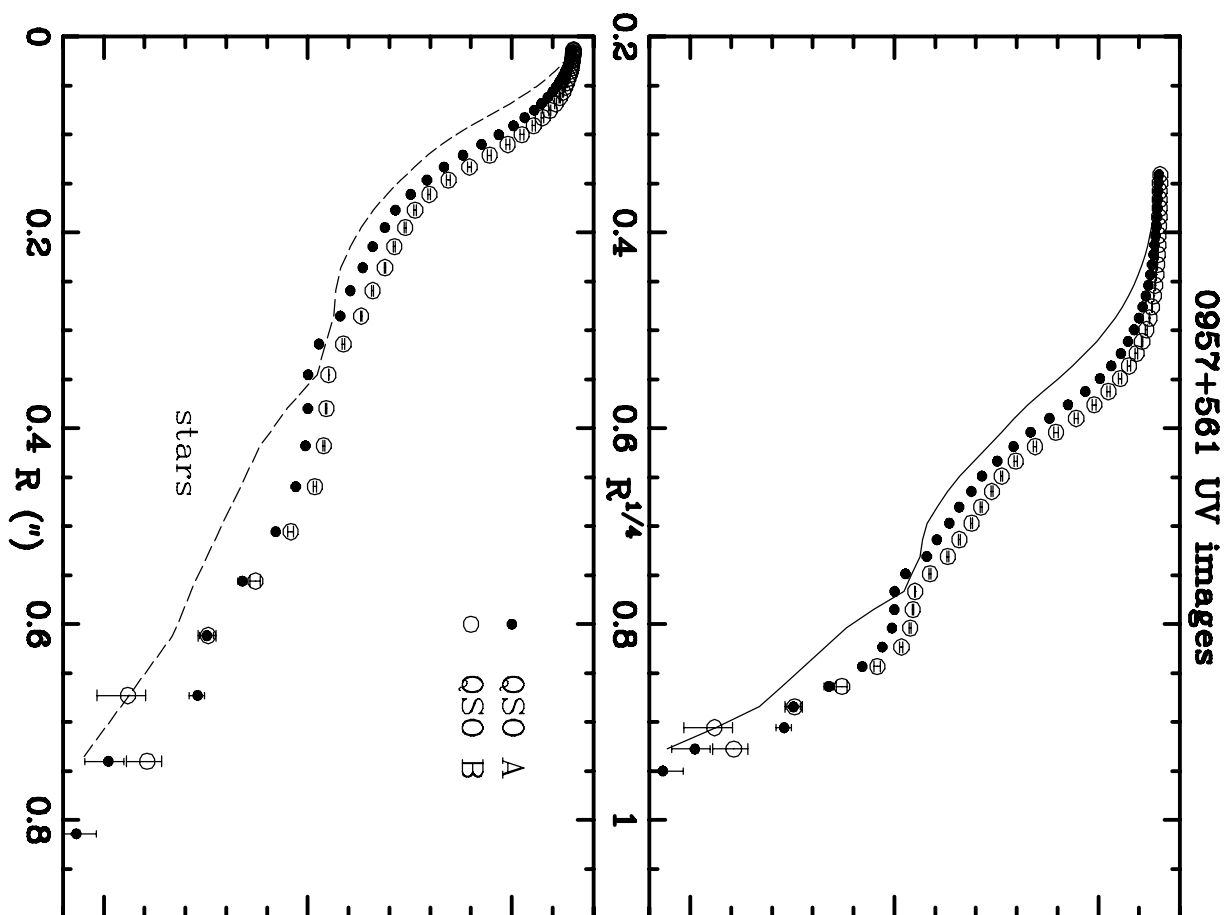
5. Cross-sections of all spectra in Table 1. The vertical dotted lines show the extraction windows for the spectra in Figure 4. The lower, slit spectra are narrower due to the slit

width. The off-nuclear spectra in Figure 6 are extracted using the light outside the inner dotted lines in the upper panel. The different dispersion orientations and uncertainties in the exact slit placement cause the different amounts of off-nuclear light.

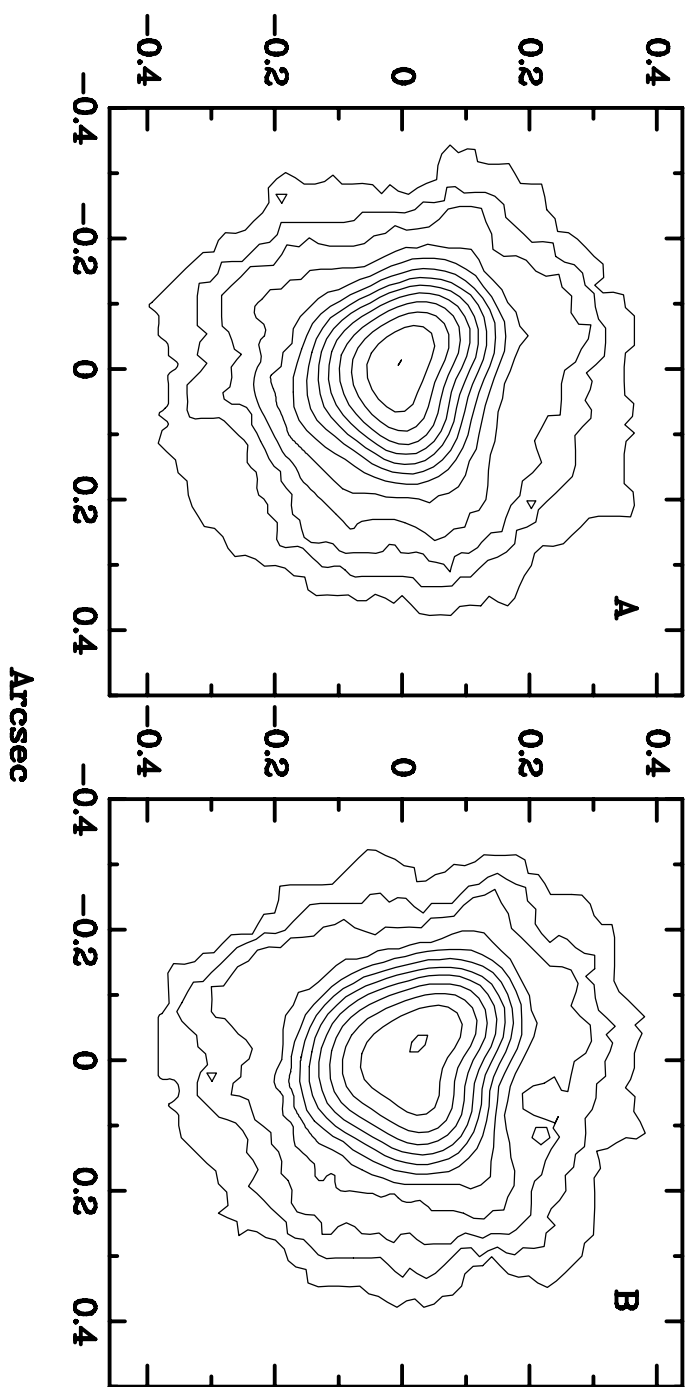
6. Panel of Ly $\alpha$  emission separately for the two QSO images. These spectra are normalised to a continuum fitted to the entire UV spectrum in all cases. The upper four (dashed) spectra are from the slitless data. Note the Ly $\alpha$  profile changes, and the possible appearance of N V away from the nucleus.



# Magnitudes



0957+561 UV images



0957+561 A+B

